

# HIGH ORDER SLIDING MODE OBSERVER BASED BACKSTEPPING CONTROL DESIGN FOR PWM AC/DC CONVERTER

M. TAHAR K. ZEMALACHE MEGUENNI A. OMARI

Electrotechnics Department, Faculty of Electrical Engineering  
University of Sciences and Technology of Oran. Mohamed Boudiaf (USTO-MB).  
[mrtahar@hotmail.com](mailto:mrtahar@hotmail.com).

**Abstract:** *In this paper, a full-bridge boost power converter topology is studied for power factor control, using nonlinear backstepping technique based on the Virtual Flux Oriented Control BVFOC. The proposed control forces the input currents to track the desired values, which can control the output voltage while keeping the power factor close to one. High Order Sliding Mode Observer (HOSMO) is employed to estimate the AC phase voltage and load current only from the measurement input currents. Lyapunov analysis shows the asymptotic convergence of the closed loop system to zero. Simulation results show the effectiveness and robustness of the proposed controller.*

**Key words:** *PWM AC DC converter, Backstepping control, High Order Sliding Mode Observer, Virtual Flux Oriented Control.*

## 1. Introduction.

Traditionally, diode or thyristor bridge rectifiers are extensively employed in industrial fields and consumer products to obtain DC voltage from AC main. This has the advantages of being simple, robust, and inexpensive. However, these rectifiers result in only unidirectional power flow and pollute the utility with low-order harmonics, which are difficult to filter. Apart from application of active and passive filters, a Pulse Width-Modulated (PWM) rectifier is used to overcome this problem. It offers several advanced features such as low harmonic distortion of input currents, bidirectional power delivery capability, high power factor, and high-quality DC-bus voltage with small filter circuit. Moreover, it represents an interesting solution for equipment which frequently works in regeneration operation, like adjustable speed drives (ASDs) and for the integration of renewable energy applications [1-2].

After significant achievements in subject of the power inversion much attention has been paid to the problem of rectification. The control strategies for the PWM rectifiers have been adapted from the methods elaborated for the vector control of the induction motors. These methods are mostly based on field-orientation methodology using linear PI controllers [3]. The inconveniences of the mentioned techniques are complicated ways of setting up of the linear controllers and the necessity of the strict knowledge of the values of the line and load parameters. This is due to the fact

that the PI control performance is strictly dependent on the proper identification of the line chokes inductance and the DC-link capacitance. Thus a disadvantage of the linear control is the sensitiveness of the converter's control system to the variations of the line and load parameters.

Recently more stress has been put on the elaboration of the nonlinear control algorithms for the PWM rectifiers in order to eliminate the disadvantageous influence of the variations of the line and load parameters on the converter operation. The significant advantage of the nonlinear control methods is no need for strict knowledge about the controlled plant, the high robustness of the control system to variations of the power circuit parameters and to disturbances like the load changes [4-6].

Due to new developments in nonlinear control theory, several nonlinear control techniques have been introduced in the last two decades, such as input-output linearization [7], feedback linearization [8], fuzzy logic control [9], passivity-based control [10], backstepping technique control [11], Lyapunov-based control [12-13], differential flatness based control [14-15], and sliding mode control [16-18]. However, most of the above works need continuous measurements of AC voltages, AC currents and DC voltage. This requires a large number of both voltage and current sensors, which increases system complexity, cost, space, and reduces system reliability. Moreover, the sensors are susceptible to electrical noise, which cannot be avoided during high-power switching. Reducing the number of sensors has a significant an exact upon the control system's performance [19-20].

The objective of this paper is to design an efficient AC/DC power converter with unity power factor, by eliminating the using of phase voltage and load currents sensors. High Order Sliding Mode Observer (HOSMO) is designed to observe the phase voltage and load current from the measured output voltage. The proposed HOSMO guarantees fast convergence rate of the observation error dynamics, facilitating the design of controllers.

The paper is organized as follows. In Section 2, the mathematical model is presented. In section 3 the development of the nonlinear backstepping controller

design for PWM rectifier is described. In Section 4, High order sliding mode observer to estimate the AC phase voltage and load current is presented. In Section 5, simulations results of the performance of the obtained backstepping control are presented. Finally, some conclusions are drawn in Section 6.

## 2. Mathematical model for PWM AC/DC converter

Figure 1 represents the topology of the converter under study. The dynamic model of PWM AC-DC converter in rotating frame d-q is given by [8-21].

$$\begin{cases} \frac{di_{sd}}{dt} = -\frac{R_s}{L_s}i_{sd} + \omega i_{sq} + \frac{1}{L_s}(v_{sd} - v_d) \\ \frac{di_{sq}}{dt} = -\frac{R_s}{L_s}i_{sq} - \omega i_{sd} + \frac{1}{L_s}(v_{sq} - v_q) \\ \frac{dv_{dc}}{dt} = \frac{3}{2cv_{dc}}(v_{sd}i_{sd} + v_{sq}i_{sq}) - \frac{i_L}{C} \end{cases} \quad (1)$$

Where  $i_{sd}$ ,  $i_{sq}$ ,  $v_{sd}$  and  $v_{sq}$  are the line current ( $i_{sa}$ ,  $i_{sb}$ ,  $i_{sc}$ ) and phase voltages ( $v_{sa}$ ,  $v_{sb}$ ,  $v_{sc}$ ) transformed to the d-q reference frame,  $v_{dc}$  is the DC-voltage and  $i_L$  is the load current,  $v_d$  and  $v_q$  are (d-q) axis converter input voltage.  $R_s=(r_r + r_p)$  and  $L_s=(l_r + l_p)$  mean the line resistance and inductance respectively.

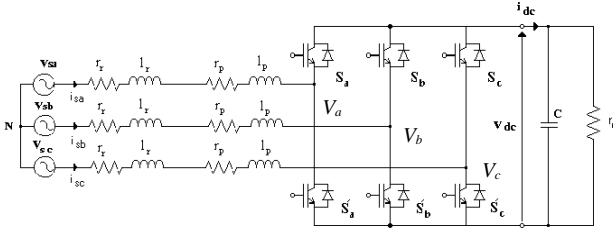


Fig. 1. Structure of voltage source PWM AC / DC converter

## 3. Backstepping Virtual Flux Oriented Control

The control techniques of the converter's current vector originate from the field oriented control approach for the induction motor under the assumption that the grid phase voltage  $v_s$ , line resistance  $R_s$  and inductance  $L_s$  are considered to be a three-phase virtual induction machine. The principles of the Backstepping Virtual Flux Oriented Control for the PWM rectifier is the decomposition of the grid current vector is based on the Park transformations into the two components  $i_{sd}$  and  $i_{sq}$  in the (d-q) coordinate frame oriented with the virtual grid flux vector as depicted in figure 2.

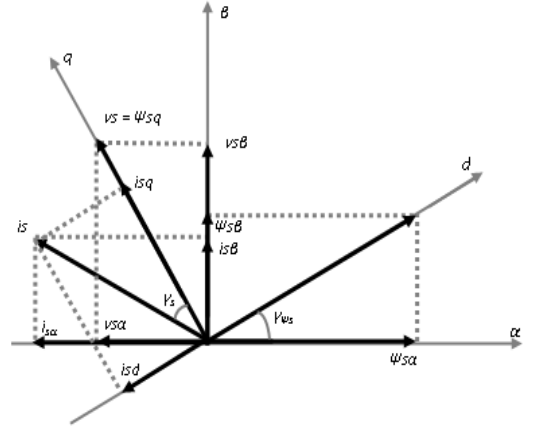


Fig. 2. Vector diagram of virtual grid flux vector orientation method.

In stationary reference frame ( $\alpha$ ,  $\beta$ ), the components of virtual line flux are estimated by integration of the corresponding voltage vector components as follows:

$$\hat{\Psi}_s = \begin{bmatrix} \hat{\Psi}_{s\alpha} \\ \hat{\Psi}_{s\beta} \end{bmatrix} = \begin{bmatrix} \int \hat{v}_{s\alpha} dt \\ \int \hat{v}_{s\beta} dt \end{bmatrix} \quad (2)$$

The estimated line voltages in the ( $\alpha$ - $\beta$ ) is given by the sum of the voltage reference of the PWM rectifier ( $v_{\alpha}$ ,  $v_{\beta}$ ) and the estimated inductor voltage (the resistive filter parameter can be neglected).

Based on the measured DC-link voltage  $v_{dc}$  and the converter switch state  $S_a$ ,  $S_b$ ,  $S_c$  the rectifier input voltages are estimated as flows

$$\begin{bmatrix} \hat{v}_{\alpha} \\ \hat{v}_{\beta} \end{bmatrix} = \begin{bmatrix} \sqrt{\frac{2}{3}}v_{dc} \left( S_a - \frac{1}{2}(S_b + S_c) \right) \\ \frac{1}{\sqrt{2}}v_{dc} (S_b - S_c) \end{bmatrix} \quad (3)$$

Then, the virtual flux  $\hat{\Psi}_s$  components are calculated from (2) in stationary coordinates system.

$$\hat{\Psi}_s = \begin{bmatrix} \hat{\Psi}_{s\alpha} \\ \hat{\Psi}_{s\beta} \end{bmatrix} = \begin{bmatrix} \int \left( \hat{v}_{\alpha} + L_s \frac{d}{dt} i_{s\alpha} \right) dt \\ \int \left( \hat{v}_{\beta} + L_s \frac{d}{dt} i_{s\beta} \right) dt \end{bmatrix} \quad (4)$$

The angular displacement of the virtual flow necessary for the Park transformation is defined as follows:

$$\begin{aligned} \sin \gamma_{\Psi_s} &= \Psi_{s\beta} / \sqrt{\Psi_{s\alpha}^2 + \Psi_{s\beta}^2} \\ \cos \gamma_{\Psi_s} &= \Psi_{s\alpha} / \sqrt{\Psi_{s\alpha}^2 + \Psi_{s\beta}^2} \end{aligned} \quad (5)$$

Since the virtual flux vector lags in respect to the grid voltage vector  $v_s$  in angle of  $\pi/2$  the reference d-

component of the current is set to zero to provide the unity power factor operation. In consequence the DC-link voltage backstepping controller provides the reference value of the q-component of the grid current. The both presented cascade control techniques provide fast dynamic response and good static performance due to the internal current control loops.

The concept of virtual flux is established to improve the Voltage Oriented Control VOC system, due to disturbances superimposed on the line voltage directly influences the coordinate transformation in the control system. Therefore, it is easier to replace the voltage angle line vector by the angle of virtual flow because it is less sensitive [22].

In the virtual flux oriented coordinates voltage equations are transformed into:

$$\begin{cases} v_{sq} = v_s = R_s i_{sq} + L_s \frac{di_{sq}}{dt} + v_q + w L_s i_{sd} \\ 0 = R_s i_{sd} + L_s \frac{di_{sd}}{dt} + v_d - w L_s i_{sq} \end{cases} \quad (6)$$

#### 4. Design of backstepping based on virtual flux oriented control.

The backstepping is a systematic and recursive design methodology for nonlinear feedback control. This approach is based upon a systematic procedure for the design of feedback control strategies suitable for the design of a large class of feedback linearisable nonlinear systems exhibiting constant uncertainty, and guarantees global regulation and tracking for the class of nonlinear systems transform-able into the parametric-strict feedback form. The backstepping design alleviates some of these limitations [23-28]. It offers a choice of design tools to accommodate uncertainties and nonlinearities and can avoid wasteful cancellations. The idea of backstepping design is to select recursively some appropriate functions of state variables as pseudo-control inputs for lower dimension subsystems of the overall system. Each backstepping stage results in a new pseudo-control design, expressed in terms of the pseudo-control designs from the preceding design stages. When the procedure terminates, a feedback design for the true control input results which achieves the original design objective by virtue of a final Lyapunov function, which is formed by summing up the Lyapunov functions associated with each individual design stage [29-30].

##### 4.1 Design of backstepping control system based on virtual grid flux

The backstepping design procedure consists of the following steps:

Step 1: Direct current controller:

Let us define the direct current error as  $e_d = i_{sd} - i_{sdref}$  and the derivative according to the time as  $\dot{e}_d = (\dot{i}_{sd} - \dot{i}_{sdref})$ .

$$\dot{e}_d = \dot{i}_{sd} = -\frac{R_s}{L_s} i_{sd} + w i_{sq} - \frac{1}{L_s} v_d \quad (7)$$

Then accounting equation (6) implies:

$$\dot{e}_d = \dot{i}_{sd} = -\frac{R_s}{L_s} i_{sd} + w i_{sq} - \frac{1}{L_s} v_d \quad (8)$$

The Lyapunov candidate function given as:

$$V_1 = \frac{1}{2} e_d^2 \quad (9)$$

If this function is always positive and its derivative is always negative, then the error will be stable and tend towards zero. The derivative of the function is written as:

$$\dot{V}_1 = e_d \dot{e}_d \quad (10)$$

In order that the derivative of the test is still negative, it must take the derivative of the form  $\dot{V}_1 = -K_1 e_d^2$  where  $K_1$  is a positive design parameter introduced by the backstepping method, which must always be positive and nonzero to meet the stability criteria of Lyapunov function. In addition, this parameter can influence the dynamics of regulation.

$$\dot{V}_1 = -K_1 e_d^2 + e_d \left( K_1 e_d - \frac{R_s}{L_s} i_{sd} + w i_{sq} - \frac{v_d}{L_s} \right) \quad (11)$$

In order to have  $\dot{V}_1 = -k_1 e_d^2 \leq 0$  (Semi-defined negative) it must be:

$$K_1 e_d - \frac{R_s}{L_s} i_{sd} + w i_{sq} - \frac{v_d}{L_s} = 0 \quad (12)$$

We obtain:

$$v_d = L_s \left( K_1 e_d - \frac{R_s}{L_s} i_{sd} + w i_{sq} \right) \quad (13)$$

Step2: The proposed of this control design is to achieve the reference DC-voltage tracking. The definition of tracking error is as follows:

$$e_v = v_{dc} - v_{dcref} \quad (14)$$

Deriving  $e_v$  according to the time as:

$$\dot{e}_v = \dot{v}_{dc} - \dot{v}_{dcref} \quad (15)$$

$$\dot{e}_v = \frac{3}{2Cv_{dc}} v_{sq} i_{sq} - \frac{i_L}{C} \quad (16)$$

In order to make the voltage tracking error tends to zero, Lyapunov function is constructed for the subsystem (14).

$$V_2 = \frac{1}{2} e_v^2 \quad (17)$$

Its derivative along the solution of (17), is given by:

$$\dot{V}_2 = e_v \dot{e}_v \quad (18)$$

$$\dot{V}_2 = e_v \left( \frac{3v_{sq}}{2Cv_{dc}} i_{sq} - \frac{i_L}{C} \right) \quad (19)$$

Utilizing the backstepping design method, we consider the q axe current component  $i_{sq}$  and as our virtual

control elements and specify its desired behavior, which are called stabilizing function in the backstepping design terminology as follows:

$$i_{sqref} = \frac{2Cv_{dc}}{3v_{sq}} \left( \frac{i_L}{C} - K_2 e_v \right) \quad (20)$$

Where  $K_2$  is positif constant.

Substituting (20) in (19) the derivative of  $V_2$  becomes:

$$\dot{V}_2 = -K_2 e_v^2 \leq 0 \quad (21)$$

### Step 3: Quadratic current error

In practice, the quadratic current  $i_{sq}$  is not equal to the desired value. Let us define the quadratic current error as  $e_q = i_{sq} - i_{sqref}$  and the derivative according to the time as

$$\begin{aligned} \dot{e}_q = & -\frac{R_s}{L_s} i_{sq} - w i_{sd} + \frac{1}{L_s} (v_{sq} - v_q) - \\ & \frac{2C}{3v_{sq}} \left[ \left( -2K_2 v_{dc} + K_2 v_{dcref} + \frac{i_L}{C} \right) \dot{v}_{dc} + \frac{i_L}{C} v_{dc} \right] \end{aligned} \quad (22)$$

To analyze the stability of this system we propose the following Lyapunov function:

$$V_T = \frac{1}{2} (e_d^2 + e_v^2 + e_q^2) \quad (23)$$

Its derivative is:

$$\dot{V}_T = e_d \dot{e}_d + e_v \dot{e}_v + e_q \dot{e}_q \quad (24)$$

$$\begin{aligned} \dot{V}_T = & -k_1 e_d^2 - k_2 e_v^2 - k_3 e_q^2 + e_q \left( k_3 e_q - \frac{R_s}{L_s} i_{sq} - \right. \\ & \left. \frac{2C}{3v_{sq}} \left[ \left( -2K_2 v_{dc} + K_2 v_{dcref} + \frac{i_L}{C} \right) \dot{v}_{dc} + \frac{i_L}{C} v_{dc} \right] \right) \end{aligned} \quad (25)$$

The expression (25) found above requires the following control laws:

$$\begin{aligned} v_q = & L_s \left( K_3 e_q - \frac{R_s}{L_s} i_{sq} - w i_{sd} + \frac{v_{sq}}{L_s} - \right. \\ & \left. \frac{2\dot{v}_{dc}}{3v_{sq}} \left( i_L + CK_2 v_{dcref} \right) + \frac{4CK_2}{3v_{sq}} v_{dc} \dot{v}_{dc} - \frac{2i_L}{3v_{sq}} v_{dc} \right) \end{aligned} \quad (26)$$

With this choice the derivatives of (23) become:

$$\dot{V}_T = -K_1 e_d^2 - K_2 e_v^2 - K_3 e_q^2 \leq 0 \quad (27)$$

## 5. High Order Sliding Mode Current Observer for Virtual Grid Flux

The technique of higher order sliding mode has been introduced in the 80s by Emelyanov. This technique not only has good properties of robustness with respect to parametric uncertainties, the modeling errors and disturbances, but also the simplicity of implementation of classical sliding mode. Its remarkable advantage is that it allows the reduction of the chattering

phenomenon, while maintaining performance system. Furthermore, in the case of higher-order sliding modes and unlike the conventional sliding mode, the discontinuity is no longer on the first derivative of the slip variable, but on a higher order derivative. This observer can reconstruct the non-measurable variables from measurements available state.

$$\begin{cases} \frac{di_{s\alpha}}{dt} = -\frac{R_s}{L_s} i_{s\alpha} + \frac{1}{L_s} (v_{s\alpha} - v_\alpha) \\ \frac{di_{s\beta}}{dt} = -\frac{R_s}{L_s} i_{s\beta} + \frac{1}{L_s} (v_{s\beta} - v_\beta) \\ \frac{dv_{s\alpha}}{dt} = -w v_{s\beta} \\ \frac{dv_{s\beta}}{dt} = -w v_{s\alpha} \end{cases} \quad (28)$$

These equations can be represented under the form

$$\begin{aligned} \dot{X}_1 &= X_2 + \phi(U, Y) \\ \dot{X}_2 &= F(X_1, X_2) \end{aligned} \quad (29)$$

$$\begin{aligned} \text{Where } X_1 &= [i_{s\alpha} \ i_{s\beta}]^T, \quad X_2 = \left[ \frac{1}{L_s} v_{s\alpha} \ \frac{1}{L_s} v_{s\beta} \right]^T, \\ U &= [v_\alpha \ v_\beta]^T \quad \phi(U, Y) = \left[ -\frac{R_s}{L_s} X_1 - \frac{1}{L_s} U \right], \\ F(X_1, X_2) &= [-w \cdot v_{s\beta} \ w \cdot v_{s\alpha}]^T \end{aligned}$$

The observer based on the super twisting algorithm for the system (29) can be designed as follows:

$$\begin{cases} \dot{\hat{X}}_1 = \hat{X}_2 + \phi(U, Y) + \alpha_2 \lambda(\tilde{X}_1) \text{sing}(\tilde{X}_1) \\ \dot{\hat{X}}_2 = F(\hat{X}_1, \hat{X}_2) + \alpha_1 \text{sign}(\tilde{X}_1) \end{cases} \quad (30)$$

Where  $\alpha_1$  and  $\alpha_2$  the observer gains. These gains are defined as follows:

$$\alpha_1 = \begin{bmatrix} \alpha_{1,1} & 0 \\ 0 & \alpha_{1,2} \end{bmatrix} \quad \alpha_2 = \begin{bmatrix} \alpha_{2,1} & 0 \\ 0 & \alpha_{2,2} \end{bmatrix}$$

We define  $\tilde{X}_1$  the error between the actual and the estimated state as:

$$\tilde{X}_1 = X_1 - \hat{X}_1 = \begin{bmatrix} X_{1,1} - \hat{X}_{1,1} \\ X_{2,1} - \hat{X}_{2,1} \end{bmatrix} = \begin{bmatrix} i_{s\alpha} - \hat{i}_{s\alpha} \\ i_{s\beta} - \hat{i}_{s\beta} \end{bmatrix} \quad (31)$$

$$\lambda(\tilde{X}_1) = \begin{bmatrix} |X_{1,1} - \hat{X}_{1,1}|^{\frac{1}{2}} & 0 \\ 0 & |X_{2,1} - \hat{X}_{2,1}|^{\frac{1}{2}} \end{bmatrix} \quad (32)$$

$$\text{sign}(\tilde{X}_1) =$$

$$\begin{bmatrix} \text{sign}(X_{1,1} - \hat{X}_{1,1}) & 0 \\ 0 & \text{sign}(X_{2,1} - \hat{X}_{2,1}) \end{bmatrix} \quad (33)$$

In the real applications the line voltage distortions occur relatively often due to the pulsed currents drawn by the nonlinear loads.

The virtual flux vector is far less sensitive to the line disturbances and maintains near sinusoidal shape even in case of the low-harmonic pollution in the supply voltage. In order to achieve a smooth estimate of the virtual grid flux, the line voltage estimated should be directly integrated as follows [6, 22]:

$$\hat{\Psi}_s = \begin{bmatrix} \hat{\Psi}_{s\alpha} \\ \hat{\Psi}_{s\beta} \end{bmatrix} = \begin{bmatrix} \int Ls \hat{X}_{2,1} dt + \hat{\Psi}_{s\alpha 0} \\ \int Ls \hat{X}_{2,2} dt + \hat{\Psi}_{s\beta 0} \end{bmatrix} \quad (34)$$

### 5.1 Load current estimation

In this work, the load current is considered as perturbation denoted  $d = -\frac{i_L}{C}$ .

The last differential equation in (1) is used to construct the observer dynamics using HO sliding mode technique defined by:

$$\frac{dv_{dc}}{dt} = \frac{3}{2Cv_{dc}} (v_{sd}i_{sd} + v_{sq}i_{sq}) - \frac{i_L}{C} \quad (35)$$

These equations can be represented under the form

$$\begin{cases} \dot{X}_3 = A_3 X_3 + B_3 U_3 + d \\ Y_3 = C_3 X_3 \end{cases} \quad (36)$$

Where

$$X_3 = [v_{dc} \ d]^T, \quad U_3 = [i_{sq}] \quad , \quad A_3 = \begin{bmatrix} 0 & 1 \\ 0 & 0 \end{bmatrix}$$

$$B_3 = \begin{bmatrix} \frac{3v_{sq}}{2Cv_{dc}} \\ 0 \end{bmatrix}, \quad d = \begin{bmatrix} 0 \\ -\frac{1}{C} \frac{di_L}{dt} \end{bmatrix}, \quad C_3 = [1 \ 0]$$

The observer becomes:

$$\begin{cases} \dot{\hat{X}}_3 = A_3 \hat{X}_3 + B_3 U_3 + \alpha_3 \lambda (Y_3 - \hat{Y}_3) + \alpha_4 (Y_3 - \hat{Y}_3) \\ \hat{Y}_3 = C_3 \hat{X}_3 \end{cases} \quad (37)$$

Where

$$\alpha_3 \lambda (Y_3 - \hat{Y}_3) = \begin{bmatrix} \alpha_{3,1} |Y_3 - \hat{Y}_3|^{\frac{1}{2}} \text{sign}(Y_3 - \hat{Y}_3) \\ \alpha_{3,2} \text{sign}(Y_3 - \hat{Y}_3) \end{bmatrix} \quad (38)$$

$$\alpha_4 (Y_3 - \hat{Y}_3) = \begin{bmatrix} \alpha_{4,1} \\ 0 \end{bmatrix} (Y_3 - \hat{Y}_3) \quad (39)$$

Where  $\alpha_3$  and  $\alpha_4$  the observer gains. These gains are defined as follows:

$$\alpha_3 = \begin{bmatrix} \alpha_{3,1} \\ \alpha_{3,2} \end{bmatrix}, \quad \alpha_4 = \begin{bmatrix} \alpha_{4,1} \\ 0 \end{bmatrix}$$

The observation error is defined by:

$$\tilde{X}_3 = X_3 - \hat{X}_3 = \begin{bmatrix} \tilde{Y}_3 \\ \tilde{d} \end{bmatrix} = \begin{bmatrix} Y_3 - \hat{Y}_3 \\ d - \hat{d} \end{bmatrix} \quad (40)$$

Leading to the dynamics:

$$\dot{\tilde{X}}_3 = \dot{X}_3 - \dot{\hat{X}}_3 = (A_3 - \alpha_4 C_3) \tilde{X}_3 + \mathbf{d} + \alpha_3 \lambda(\tilde{Y}_3) \quad (41)$$

Under the assumption that the derivative of  $i_L$  is bounded (i.e.  $|\frac{di_L}{dt}|_{max} < \Pi_{i_L}$ ) where  $\Pi_{i_L}$  is a positive constant, the finite time convergence of the observer is guaranteed choosing the gains  $\alpha_3$  and  $\alpha_4$  satisfying the conditions of the Lyapunov function. Thus after finite time, one has  $\dot{\tilde{X}}_3 = \tilde{X}_3 = 0$ , leading to the estimation of load current.

### 6. Simulation Results

In order to confirm the effectiveness of the proposed HOSM observer based BVFOC scheme and evaluate its performance under different conditions, a model of three-phase PWM rectifier, including the control system is presented in Fig.3.

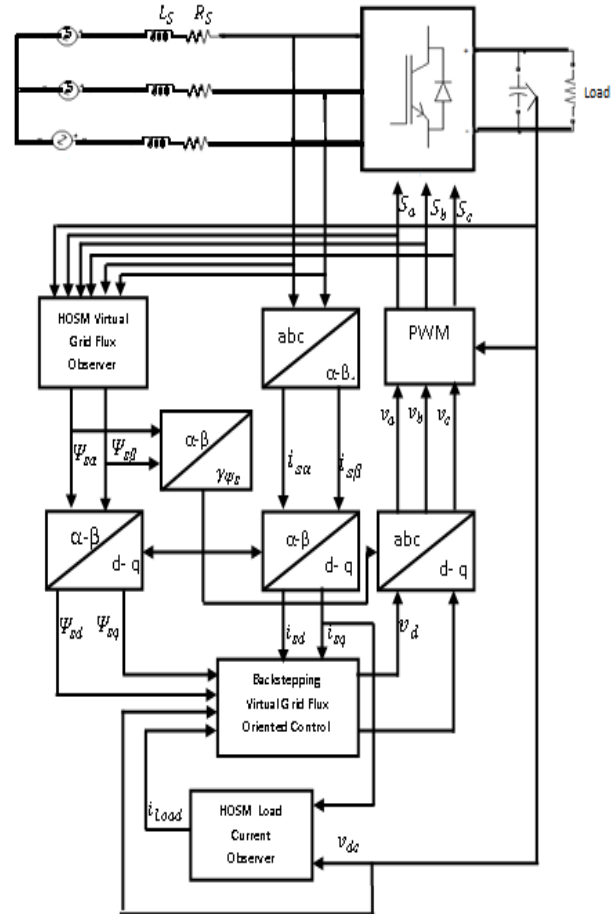


Fig. 3. Sensorless Backstepping Virtual Flux Oriented Control.

The main parameters used in the simulation, are tabulated in Table 1 and 2.

Table 1: Main parameters used in Simulation

phase voltage ( peak) $V_s$	120 V
Source voltage frequency $f_s$	50 Hz
Line resistance $R_s$	0.5 $\Omega$
Line inductor $L_s$	6 mH
DC-bus capacitor C	1000 $\mu$ F
Load resistance $R_l$	20 $\Omega$
Switching frequency $f_c$	5 KHz
DC-bus voltage $v_{dc}$	200 V

Table 2: Controllers and observer gains

$K_1$	$K_2$	$K_3$	$\alpha_{1,1}$	$\alpha_{1,2}$	$\alpha_{2,1}$	$\alpha_{2,2}$	$\alpha_{3,1}$	$\alpha_{3,2}$	$\alpha_{4,1}$
10000	7000	9000	-500	-100	-500	-100	20	2	1

The simulations results of the proposed observer (HOSM) based backstepping virtual flux oriented control are shown in fig (4-8). Input phase current along with corresponding source voltage are shown in fig.4. From this figure make no phase shift between the input current and corresponding source voltage.

Figure 5 presents the transients of the line current in the (d-q) coordinate frame under the step change of the converter load. The converter fulfills the unity power factor condition,  $i_{sd} = 0$ , while the flow of the active line current component  $i_{sq}$  is forced. Figure 6 shows the output voltage performance of the AC/DC converter. From this figure, it is seen that the proposed observer-based backstepping virtual flux oriented control is able

to regulate the output voltage to the desired level under the condition of load variation.

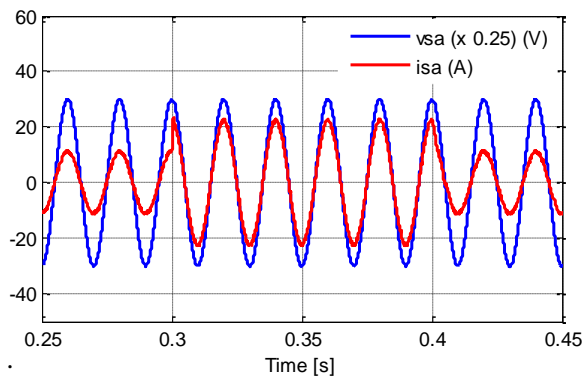


Fig. 4. Line voltage and line current under the step change of the converter load

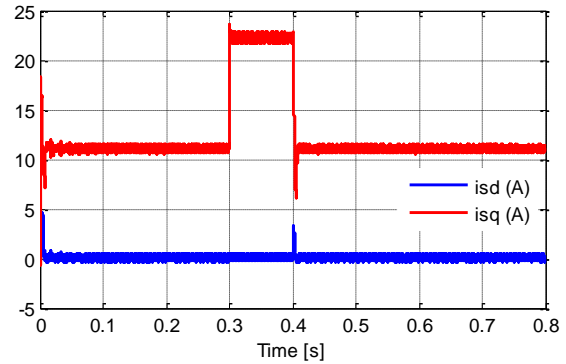


Fig.5 . d-q components of line current under the step change of the converter load

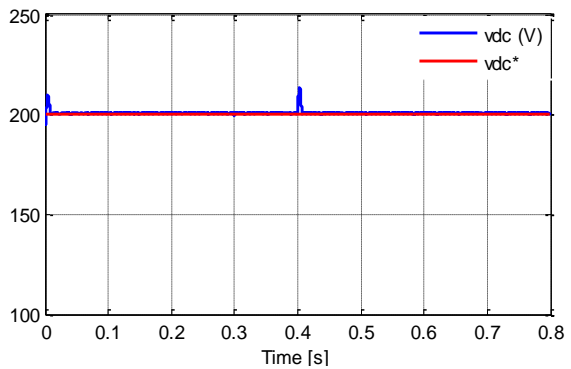


Fig. 6. Output voltage

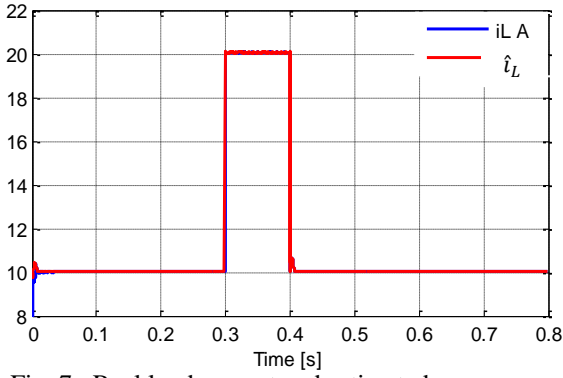


Fig. 7. Real load current and estimated.

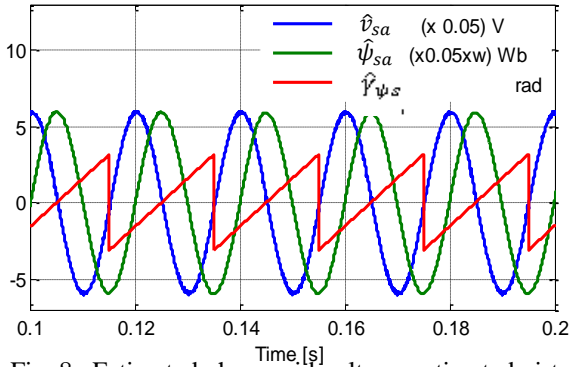


Fig. 8. Estimated phase grid voltage, estimated virtual grid flux and angle of position of virtual grid flux vector.

### 6.1 Robustness to parameter mismatches

In this section an examination of the robustness of the proposed high order sliding mode current observer for the virtual grid flux and load current observer to the parameter mismatches will be carried out.

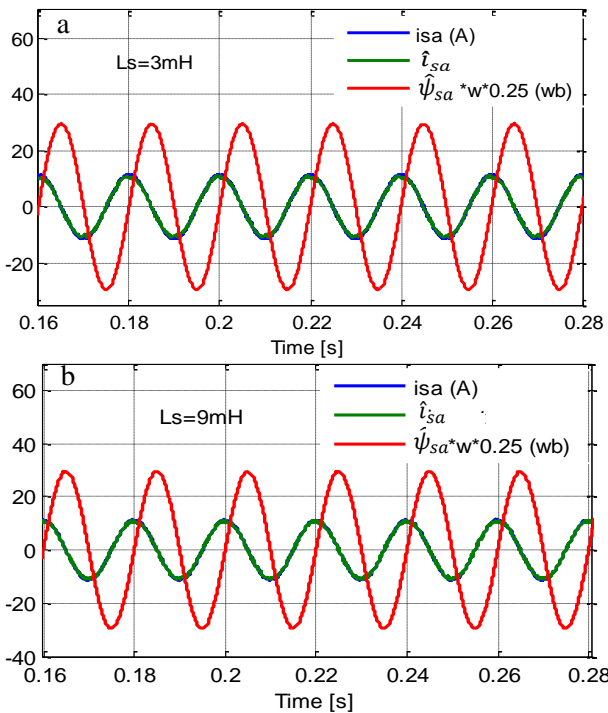


Fig. 9. Examination of robustness to changes values of input filter inductance  $L_s$ .

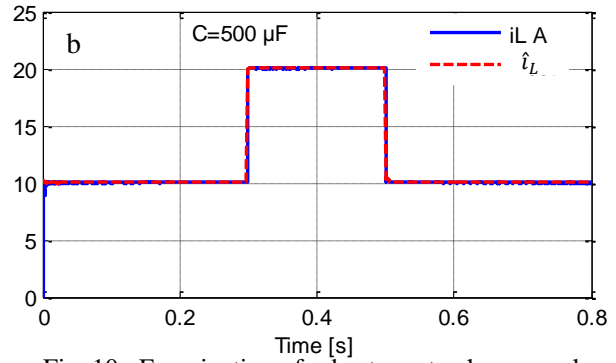
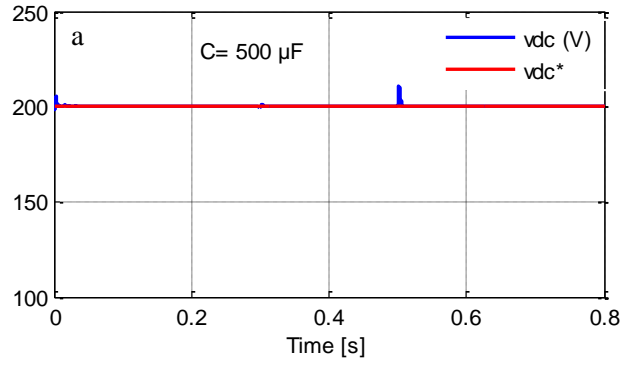


Fig. 10. Examination of robustness to changes values of output capacitance  $C$ .

The insensitiveness of the HOSMO technique to the changes of the values of the inductance of the input line filter ( $L_s$ ) as presented in Fig.9 a,b. The system performance was not much affected by the change.

The robustness test, an output capacitance variation of -50% under the step change of the load rectifier is carried out. This case is represented by Fig. (10a) and (10b) for the DC link voltage, and load current estimation respectively. The results reveal the efficiency of the proposed observer controller scheme.

### 7. Conclusion

This paper has presented the development of a new Backstepping virtual flux oriented control scheme with HOSMO for three-phase PWM rectifier. The use of observer reduces the number of sensors, decrease the system cost, volume and provide robustness to the change of operational condition. The main goal of the proposed control strategy is to achieve near-sinusoidal input current waveforms of the converter under different conditions and maintaining the DC-bus voltage at the required level. Simulation results have proven excellent performance of the proposed BVFOC scheme, even in both transient and steady states. Nearly sinusoidal waveforms of input currents are successfully achieved under different conditions.

### References

1. J. R. Rodriguez, J. W. Dixon, J. R. Espinoza, and J. Pontt, P. Lezana: *PWM regenerative rectifiers:*

- state of the art, IEEE Trans. Industrial Electronics, vol. 52, No. 1, pp. 5-22 February 2005
2. R. Ghosh and G. Narayanan: *Control of three-phase, four-wire PWM rectifier*, IEEE Trans. Power Electronics, vol. 23, No. 1, pp. 96-106, January 2008.
  3. Buso S., Malesani L., Mattavelli P.: *Comparison of current control techniques for active filter application*, IEEE Trans. on Industrial Electronics, 45 No.5, 722-729, 1998.
  4. Utkin V., Guldner J., Shi J., *Sliding Mode Control in Electromechanical Systems*, Taylor & Francis 1999.
  5. Knapczyk M., Pięńkowski K.: *Real-Time Application of Virtual Flux-Based Sliding-Mode Control System of Three-Phase Boost-Type AC/DC Converter*, Control in Power Electronics and Electrical Drives SENE'07, Łódź(2007), 221-226
  6. Knapczyk M., Nonlinear control strategies of AC/DC line-side converters using sliding-mode approach. Ph. D. Diss., Wrocław Univ. of Technology, Poland, (2009)
  7. Lee, T.S., : *Input-Output Linearization and Zero-Dynamics Control of Three-Phase AC/DC Voltage-Source Converters*," IEEE Transactions on Power Electronics, 18, 11-22. (2003).
  8. Lee, D.C., Lee, G.M., and Lee, K.D. *DC-bus Voltage Control of Three-Phase AC/DC PWM Converters Using Feedback Linearization*," IEEE Transactions on Industry Applications, 36, 826-833 2000.
  9. Cecati, C., Dell'Aquila, A., Lecci, A., and Liserre, M. *Implementation Issues of a Fuzzy-Logic-Based Three-Phase Active Rectifier Employing Only Voltage Sensors*," IEEE Transactions on Industrial Electronics, 52, 378-385. 2005.
  10. Escobar, G., Chevreau, D., Ortega, R., and Mendes, E. *An Adaptive Passivity-Based Controller for a Unity Power Factor Rectifier*," IEEE Transactions on Control Systems Technology, 9, 637-644. . 2001.
  11. Allag, A., Hammoudi, M., Mimoune, S., Ayad, M., Becherif, M., and Miraoui, A. *Tracking Control Via Adaptive Backstepping Approach for a Three Phase PWM AC-DC Converter*," in IEEE International Symposium on Industrial Electronics, ISIE, pp. 371-376 2007.
  12. Pahlevaninezhad, M., Das, P., Drobnik, J., Moschopoulos, G., Jain, P., and Bakhshai, A. *A Nonlinear Optimal Control Approach Based on the Control-Lyapunov Function for an AC/DC Converter Used in Electric Vehicles*," IEEE Transactions on Industrial Informatics, 8, 596-614 . 2012a.
  13. Komurcugil, H., and Kukrer, O. *Lyapunov-Based Control for Three-Phase PWM AC/DC Voltage-Source Converters*," IEEE Transactions on Power Electronics, 13, 801-813 (1998).
  14. Pahlevaninezhad, M., Das, P., Drobnik, J., Jain, P., and Bakhshai, A. *A New Control Approach Based on the Differential Flatness Theory for an AC/DC Converter Used in Electric Vehicles*," IEEE Transactions on Power Electronics, 27, 2085-2103 (2012b).
  15. Houari, A., Renaudineau, H., Martin, J., Pierfederici, S., and Meibody-Tabar, F. *Flatness-Based Control of Three-Phase Inverter With Output Filter*," IEEE Transactions on Industrial Electronics, 59, 2890-2897 (2012).
  16. Thounthong, P. : *Control of a Three-Level Boost Converter Based on a Differential Flatness Approach for Fuel Cell Vehicle Applications*," IEEE Transactions on Vehicular Technology, 61, 1467-1472 2012.
  17. Shtessel, Y., Baev, S., and Biglari, H. : *Unity Power Factor Control in Three-Phase AC/DC Boost Converter Using Sliding Modes*," IEEE Transactions on Industrial Electronics, 55, 3874-3882, 2008.
  18. Silva, J. *Sliding Mode Control of Boost-Type Unity-Power-Factor PWM Rectifiers*," IEEE Transactions on Industrial Electronics, 46, 594-603 1999.
  19. Tan, S.C., Lai, Y., Tse, C., Martinez-Salamero, L., and Wu, C.K. *A Fast-Response Sliding-Mode Controller for Boost-Type Converters With a Wide Range of Operating Conditions*," IEEE Transactions on Industrial Electronics, 54, 3276-3286, 2007.
  20. Pu, X., Nguyen, T., Lee, D., Lee, K., and Kim, J. *Fault Diagnosis of DC-Link Capacitors in Three-Phase AC/DC PWM Converters by Online Estimation of Equivalent Series Resistance*," IEEE Transactions on Industrial Electronics, 60, p. 4118-4127 2012.
  21. [21] D.C.Lee, K.D.Lee, and G.M.Lee, "Voltage control of PWM converters using feedback linearization," IEEE Trans. Appl. conf., 2, pp. 1491-1496, 1998.
  22. KNAPCZYK M., PIĘNKOWSKI K., *Sliding-mode Virtual Flux Oriented Control of PWM rectifiers with fixed switching frequency*, Power electronics and electrical drives - selected



- problems, Wroclaw University of Technology, 2007, pp. 122–136.
23. A. R. Benaskeur, Aspects de l'application du backstepping adaptatif à la commande décentralisée des systèmes non-linéaires, PhD thesis, Department of Electrical and Computer Engineering, University of Laval, Quebec City, Canada, 2000.
  24. Tan, Y., Chang, J., Tan, H. and Hu, J., Integral Backstepping Control and Experimental Implementation for Motion System, Proceedings of the IEEE International Conference on Control Applications Anchorage, September, pp. 25\_27 (2000). Alaska, USA,
  25. Wai, R.-J., Lin, F.-J. and Hsu, S.-P., *Intelligent Backstepping Control for Linear Induction Motor Drives*, JEE Proceeding. Elect.Power Appli.Vol 148, 2001,
  26. J. Zhou, Y. Wang, *Real-time nonlinear adaptive backstepping speed control for a PM synchronous motor*, Control Engineering Practice, Vol. 13, 2005, pp. 1259-1269
  27. I. Kanellakopoulos, P.V. Kokotovic, A.S. Morse : *Systematic design of adaptive controller for feedback linearizable systems*. IEEE Trans., Auto. Control.1991. 36. (11), 1241- 1253.
  28. H. Rasmussen, P. Vadstrup, H. Borsting. : *Nonlinear decoupling of Torque and Field Amplitude of Induction Motors*. FINPIE/97 EspooFinland, 1997.
  29. T. Yaolong, J.Chang, T. Hualin. :*Adaptive Backstepping Control and Friction Compensation for AC Servo with Inertia and Load Uncerainties*. IEEE Trans. On Ind. Elect. Vol.50, No.5, 2003.
  30. M. N. Uddin, J. Lau, *Adaptive backstepping based design of a nonlinear position controller for an IPMSM servo drive*, Can. Jour. Of Elec. Comp. Eng., Vol. 32, No 2, spring 2007, pp. 97-102